Journal of Radiation Research, 2013, 54, 27–35
doi: 10.1093/jrr/rrs072 Advance Access Publication 21 August 2012

# Increased CD147 and MMP-9 expression in the normal rat brain after gamma irradiation

Hong LI[1,†], Ming WEI[1,2,*,†], Shenghui LI[2], Ziwei ZHOU[2] and Desheng XU[1]

[1]Department of Neurosurgery, the Second Hospital, Tianjin Medical University, 23 Pingjiang Road, Tianjin - 300211, China
[2]Department of Neurosurgery, General Hospital, Tianjin Medical University, 23 Pingjiang Road, Tianjin - 300211, China
[†]Ming Wei and Hong Li contributed equally to this work.
*Corresponding author. Department of Neurosurgery, the Second Hospital, Tianjin Medical University, 23 Pingjiang Road, Tianjin - 300211, China. Tel: +86-22-8832-8537; Fax: +86-22-2833-1788; Email: drweiming@163.com

(Received 22 March 2012; revised 27 June 2012; accepted 18 July 2012)

Radiation-induced vascular injury is a major complication of Gamma knife surgery (GKS). Previous studies have shown that CD147 and MMP-9 are closely associated with vascular remodeling and pathological angiogenesis. Thus, we analysed changes in CD147 and MMP-9 expression in the cerebral cortex to investigate the correlation between CD147 and MMP-9 in the rat following GKS. Adult male Wistar rats were subjected to GKS at a maximum dose of 75 Gy and then euthanized 1 to 12 weeks later. Using immunohistochemistry and western blot analysis, we found that CD147 and MMP-9 expression were markedly upregulated in the target area 8–12 weeks after GKS when compared with the control group. Immunofluorescent double staining demonstrated that CD147 signals colocalized with CD31, GFAP and MMP-9-positive cells. Importantly, CD147 levels correlated with increased MMP-9 expression in irradiated brain tissue. For the first time, these data demonstrate a potential relationship between CD147 and MMP-9 following GKS. In addition, our study also suggests that CD147 and MMP-9 may play a role in vascular injury after GKS.

**Keywords:** CD147; MMP-9; immunohistochemistry; radiosurgery; rat

## INTRODUCTION

Gamma knife surgery (GKS) is the stereotactic delivery of a single high-radiation dose as an alternative to invasive neurosurgery. The use of GKS for the treatment of vascular malformations, brain tumors, and functional brain diseases is increasing [1–3]. However, even a targeted therapeutic dose of radiation will destroy a small area of the surrounding normal tissue. This destruction will lead to a variety of histological changes similar to the vascular abnormalities often observed in central nervous system (CNS) radiation injuries, including endothelial cell swelling, vessel dilation, and changes in vascular permeability [4, 5].

CD147, a cell-surface transmembrane glycoprotein that belongs to the immunoglobulin superfamily [6], contains two extracellular immunoglobulin domains (C and V domains). CD147 promotes the formation of new blood vessels by inducing matrix metalloproteinase (MMP) production in an autocrine and paracrine manner [7] to degrade the basement membrane of damaged vessels and remodel the extracellular matrix (ECM) around neovasculature sites [8]. MMP-dependent tissue remodeling is one of the main stages of the angiogenic process. In addition to its biological benefits, increased MMP activity has been implicated in the degradation of blood-brain barrier (BBB) tight-junction proteins and increased BBB permeability [9]. These changes can lead to brain edema and hemorrhaging [10]. The correlation between CD147 expression and MMP-9 activity has been reported in many pathological processes, such as tumor occurrence, inflammation and cerebrovascular disease. For example, many studies have demonstrated that the EMMPRIN molecule is highly expressed on the surface of various malignant tumor cells and plays a pivotal role in promoting tumor invasiveness by stimulating MMP-9 production by adjacent stromal cells [11]. CD147 and MMP-9 are also believed to play a major

role in the pathogenesis of cerebral disorders, such as ischemic stroke [12] and multiple sclerosis [13]. CD147 was shown to be essential in multiple biological processes, including ECM remodeling and BBB breakdown. However, the role of CD147 and MMP-9 in CNS radiation injury remains elusive.

In this study, we investigated the effect of GKS on the expression of CD147 and MMP-9 in the rat brain. Furthermore, we correlated the overexpression of MMP-9 with CD147 expression levels in irradiated brain tissue.

## MATERIALS AND METHODS

### Animal protocol

A total of seventy-six male Wistar rats weighing between 200 and 240 g were housed individually in a temperature-(22°C) and humidity-controlled (60%) vivarium. They were maintained on a standard 12-h light/dark cycle (7:00 a.m. to 7:00 p.m.) with free access to food and water. Rats were randomly assigned to control (sham-irradiation) and GKS groups ($n = 38$ rats/group). For progression analysis, the sham-irradiation and irradiation groups were further divided into four groupsof 1, 4, 8 and 12 weeks post radiation. At each time point, four rats were used for immunohistochemistry, four rats were used for Western blot analysis, and three rats were used for Evans Blue (EB) detection and quantification. Experiments involving animals were approved by the Tianjin Medical University Animal Care and Ethics Committee.

### Gamma knife surgery

The radiation target and dose were determined based on studies described previously [14]. Briefly, each rat was anesthetized with 10% chloraldurat (3 mL/kg), and its skull was fixed in a stereotactic frame. After high-resolution MR images were obtained, the center of the irradiation area was calculated with reference to a standard rat stereotactic atlas ($X = 5$, $Y = 10$, $Z = 6.5$) [15]. A maximum dose of 75 Gy was administered in the right parietal cortex with a Leksell Gamma Knife (model C, Elekta Instrument AB, Stockholm, Sweden) using a 4-mm collimator. The control animals underwent the same procedure but did not receive any radiation.

### Histology and immunohistochemistry

The rats were perfused transcardially with 4% paraformaldehyde under intraperitoneal anesthesia. The brains were then removed and post-fixed overnight at 4°C in 4% paraformaldehyde. The radiation target was identified using the methods previously described [14]. The brains were cut at the target region, and the tissue was embedded in paraffin. Serial paraffin sections (4 μm) were cut and mounted on slides for further immunohistochemical staining. Sections were treated with standard 1.5% horse or goat serum for 30 min, followed by an overnight incubation at 4°C with goat polyclonal anti-CD147 (1:100; Santa Cruz Biotechnology, Santa Cruz, CA) and mouse monoclonal anti-MMP-9 (1:50; EMD Biosciences, Gibbstown, NJ). After incubation with biotinylated rabbit anti-goat or rabbit anti-mouse IgG for 1 h (1:100; Vector Laboratories, Burlingame, CA), the sections were incubated with ABC Reagent (Vector Laboratories, Burlingame, CA) for 30 min and visualized using 0.05% diaminobenzidine for 5–10 min. The number of positive cells in each section was quantified (400X, Leica, Wetzlar, Germany) in five fields by an investigator who was blinded to the treatment conditions. Next, the average number of positive cells per field of view was calculated. An isotype-matched negative control was used for all of the antibodies.

### EB extravasation

A 2% (w/v) solution of EB at 4 ml/kg was injected intravenously and allowed to circulate in the rats for 30 min. The brain EB extravasation was quantified spectrophotometrically. The brains were homogenized by vortexing in 250 μl of phosphate-buffered saline (PBS) for 2 min. Then, 250 μl of 60% trichloroacetic acid was added, and the samples were vortexed for an additional 2 min. After cooling for 30 min, the samples were centrifuged for 5 min at 10 000 g. Absorbance readings were measured at 620 nm. The EB extravasation results are expressed as ng of EB per mg of brain tissue. For qualitative examination of EB extravasation, the rats were perfused with 5 ml of saline followed by 5 ml of 4% paraformaldehyde. The dissected brains were immersed in 30% sucrose in 0.1M PBS for 48 h, frozen in OCT compound (Sigma Chemical Co., St. Louis, MO), and stored at –80°C. EB extravasation was observed in cryostat sections (14 μm) using a fluorescent microscope.

### Western blot analysis

Expression of CD147 and MMP-9 protein was determined for the indicated time points using western blotting. The parietal cortex (0.0–2.5 mm posterior to bregma) was collected and homogenized with RIPA buffer containing a protease inhibitor cocktail (Sigma Chemical Co., St. Louis, MO) and then incubated for 15 min on ice. The supernatant was isolated by centrifugation at 12 000 g for 20 min at 4°C. The concentration of total protein in each sample was quantified by the Bradford method (Bio-Rad, Hercules, CA), as per the manufacturer's instructions. Equal amounts of protein were separated by SDS–PAGE and then transferred to polyvinylidene difluoride membranes (Immobilon-P; Millipore, Billerica, MA) for 1 h. The membrane was blocked for 1 h and then incubated with a goat polyclonal anti-CD147 (1:200; Santa Cruz Biotechnology, Santa Cruz, CA) and polyclonal rabbit anti-MMP-9 antibody (1:1000;

Chemicon International, Temecula, CA) in blocking solution at 4°C overnight. After triple washing, the membrane was incubated with a horseradish peroxidase-conjugated secondary antibody (1:2000; Vector Laboratories, Burlingame, CA) at room temperature for 2 h. To confirm equal protein loading, the blots were also reacted with an antibody against β-actin (1:1000; Santa Cruz Biotechnology; Santa Cruz, CA). The target protein was detected using the ECL+ kit (Millipore, Billerica, MA).

## Dual fluorescence staining

For dual-immunofluorescence labeling, the cryostat sections were incubated at 4°C overnight with a goat polyclonal antibody against CD147 (1:100; Santa Cruz Biotechnology, Santa Cruz, CA), a mouse monoclonal antibody against MMP-9 (1:50; EMD Biosciences, Gibbstown), a mouse monoclonal antibody against CD31 as a marker of endothelial cells (1:50; Chemicon, Temecula, CA), a mouse monoclonal antibody against GFAP as a marker of astrocytes (1:500; Chemicon, Temecula, CA), a mouse monoclonal antibody against NeuN as a marker of neurons (1:100; Chemicon, Temecula, CA), or a rabbit polyclonal antibody against MPO as a marker of neutrophils (1:50; Abcam, Cambridge, MA). The sections were then incubated with Alexa Fluor 488-conjugated donkey anti-mouse, anti-goat, or anti-rabbit IgG and Alexa Fluor 594-conjugated donkey anti-goat IgG (1:500; Molecular Probes, Eugene, OR) at room temperature for 1 h. The slides were visualized on a fluorescent microscope. For negative controls, the primary antibody was substituted with the appropriate isotype control.

## Statistical analysis

Data are expressed as the mean ± SD. Comparisons among multiple groups were performed by an analysis of variance (ANOVA) followed by a Dunnett's *post hoc* test. Comparisons between the two experimental groups were made using Student's *t*-tests. The correlation between CD147 and MMP-9 expression was analysed by linear regression analysis. A *P*-value of less than 0.05 was considered to be statistically significant.

# RESULTS

## Radiation-induced blood brain barrier (BBB) breakdown in brain tissue

In the present study, the parietal cortex was the target of unilateral irradiation and the site of microscopic analyses. The EB extravasation into brain tissue could be visualized by red fluorescence. There was no EB extravasation observed in the irradiated brain area 1 and 4 weeks after GKS. A slight extravasation of EB dye was observed in the irradiated area 8 weeks after GKS; furthermore, this effect increased (intense red fluorescence) 16 weeks after GKS

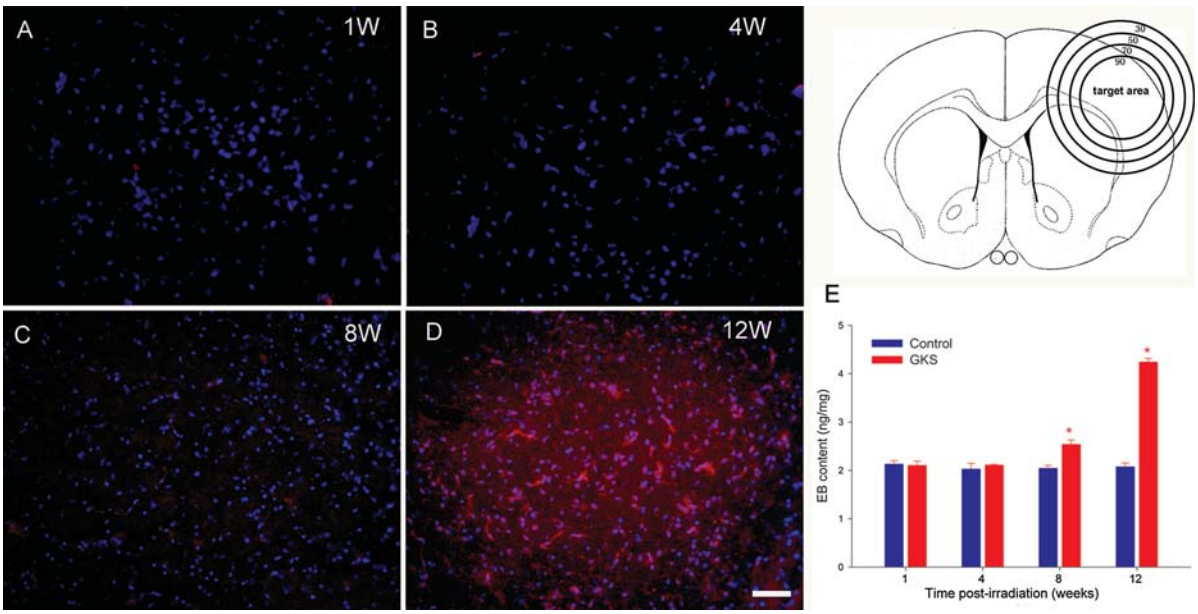


**Fig. 1.** Radiation-induced blood brain barrier (BBB) breakdown. The upper left drawing shows a coronal section of the rat brain showing the isodose curve with a maximal center dose of 75 Gy. There was no EB fluorescence detected in the irradiated cortex at 1 and 4 weeks after GKS (**A** and **B**). A weak red fluorescence was observed in the target area at 8 weeks (**C**). Significant EB fluorescence (red) was observed in the target region at 12 weeks after GKS (**D**). The EB concentration in the irradiated tissue was significantly higher than in the sham-operated group (**E**). The data are presented as the mean ± SD ($n = 3$, $^*P < 0.001$ when compared with the control group). Scale bar: 50 μm.

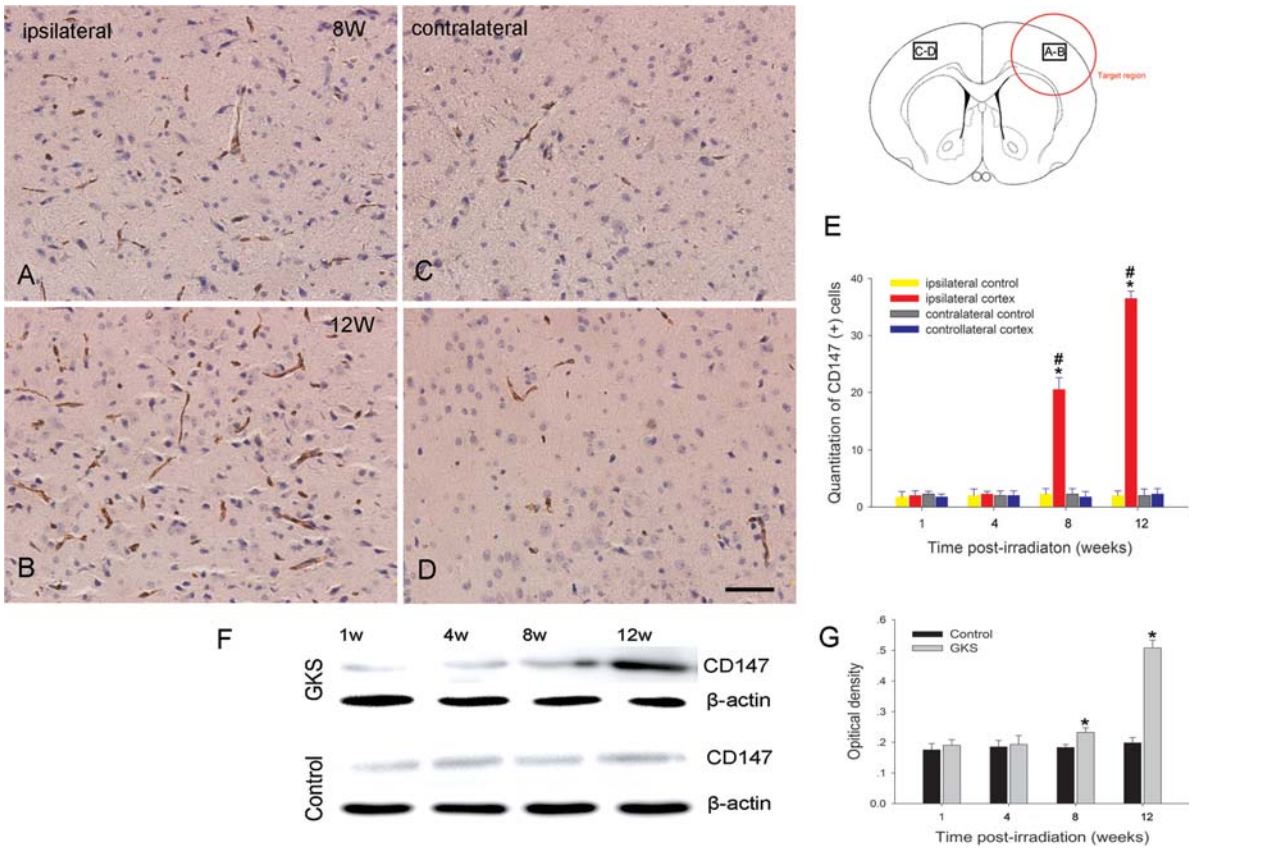


**Fig. 2.** Immunodetection of CD147 after GKS. (**A**–**D**) Representative photomicrographs of CD147 immunostaining in GKS-irradiated and non-irradiated regions. CD147 staining in the irradiated cortex (A, B) was increased when compared with the non-irradiated contralateral cortex at 8 and 12 weeks after GKS (C, D). The bar graph shows the temporal change of CD147-expressing cells after GKS (**E**). Immunoblot of CD147 protein expression in the damaged cortex after GKS (**F**). The bar graph shows the densitometric analysis of CD147-immunoreactive bands (**G**). The data are presented as the mean ± SD ($n = 4$, $^{*}P < 0.001$ when compared with the control group, $^{\#}P < 0.001$ when compared with the contralateral cortex). Scale bar: 50 μm.

(Fig. 1). Meanwhile, quantitative analysis showed that EB content in irradiated tissue was only slightly increased 8 weeks after GKS ($P < 0.001$) and elevated more than twofold 12 weeks after GKS ($P < 0.001$). No increase of EB content was observed in the irradiated tissue at 1 and 4 weeks after GKS when compared with the control tissue ($P > 0.05$).

## Expression and cellular localization of CD147 after GKS

Immunohistochemistry and western blot analysis showed that the level of CD147 protein expression was significantly higher in the irradiated tissue at 8 and 12 weeks after GKS ($P < 0.001$) when compared with the controls (Fig. 2). There was no increase in the expression of CD147 protein in the contralateral cortex of rats subjected to radiation ($P > 0.05$) when compared with the controls.

We next examined the cellular localization of CD147 by dual fluorescence staining. The results showed that CD147 is only weakly expressed in the endothelial cells of the cerebral cortex of control rats (Fig. 3). In addition, CD147 protein appeared to co-localize with CD31-positive endothelial cells and GFAP-positive astrocytes in the rat brain at 12 weeks post-irradiation. However, the CD147 signal did not co-localize with NeuN-positive neurons or MPO-positive neutrophils (Fig. 3).

## The effects of GKS on MMP-9 expression in the rat brain

Immunohistological staining showed that the number of MMP-9-positive cells was low in the brain of control rats. By comparison, the number of MMP-9-positive cells was found to be increased in the irradiated right parietal cortex 8 and 12 weeks after GKS ($P < 0.001$; Fig. 4). There was no change in the expression of CD147 protein in the non-irradiated left parietal cortex ($P > 0.05$) when compared with the control.

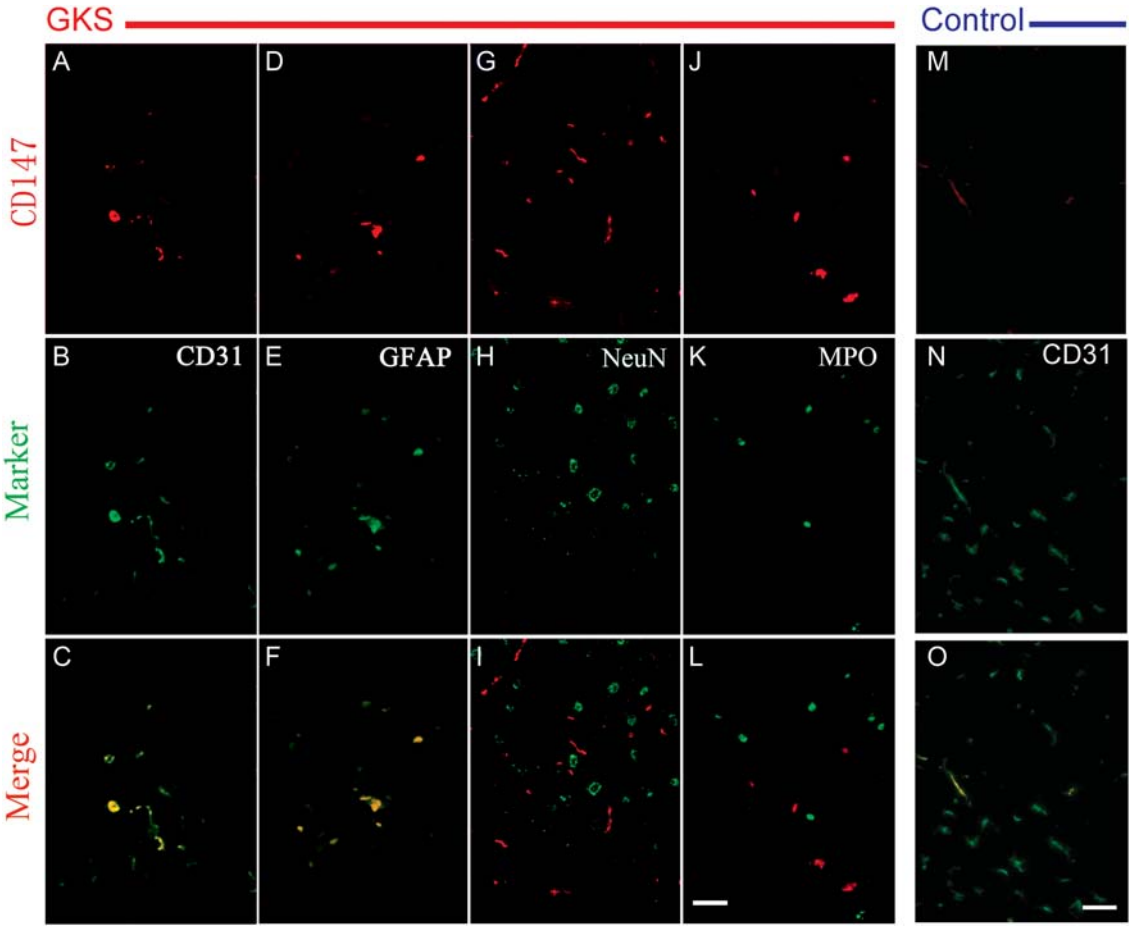


**Fig. 3.** Representative photomicrographs of double fluorescent staining of CD147 with different cell markers in the irradiated brain tissue. Brain sections were stained for CD147 (red), CD31 (green), GFAP (green), and MPO (green). Co-localization of red and green fluorescence is shown in yellow. CD147+ cells are colocalized with CD31+ endothelial cells and GFAP+ astrocytes in the irradiated tissue. CD147+ cells are only colocalized with CD31+ endothelial cells in the control tissue. Scale bar: 50 μm.

To further examine the upregulation of MMP-9, proteins obtained from homogenates of rat brain tissue were used for western blot analysis. The MMP-9 protein level was significantly higher in the rat brain at 8 and 12 weeks after GKS when compared with the control ($P < 0.001$; Fig. 4). There was no difference between the rats in the radiation groups and the control rats at 1 and 4 weeks after GKS ($P > 0.05$).

### The association between CD147 and MMP-9 expression in the parietal cortex after GKS

To further understand the relationship between CD147 and MMP-9 expression in the irradiated brain, we used a double-immunofluorescence technique to investigate the localization of CD147 and MMP-9 after GKS. The results showed that CD147 colocalized with MMP-9 in the vascular lumen-like structure in the GKS group 12 weeks after GKS (Fig. 5). In addition, MMP-9 expression was significantly correlated with CD147 expression using linear regression correlation analysis ($R^2 = 0.834$, $P < 0.001$). These data suggest that enhanced expression of CD147 may increase MMP-9 levels in irradiated brain tissues.

## DISCUSSION

Irradiation of the right parietal cortex was accomplished using the Gamma Unit C model of the Leksell stereotactic system, and targeting accuracy was confirmed [14]. According to published radiobiological studies, an intermediate dose of focal gamma-irradiation elicits vascular alterations at 3 months post-irradiation without necrosis [14]. Similar results were observed in the present study, where rats subjected to experimental GKS showed an increase in vascular permeability. The effects of gamma irradiation on vascular injury remain unclear, but an increasing body of literature regarding CNS radiation injury suggests that modifying factors associated with tissue remodeling and angiogenesis, such as VEGF and FGF, can

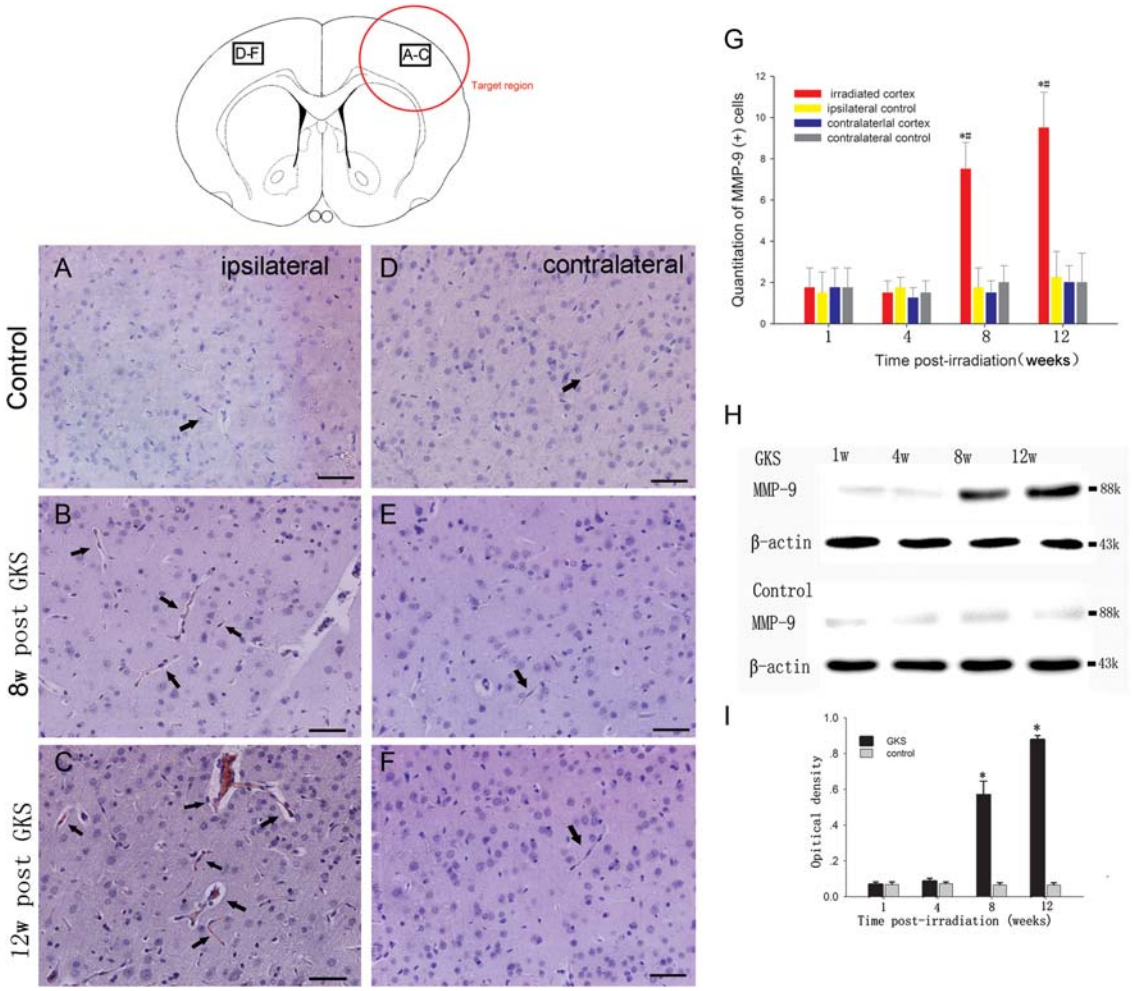


**Fig. 4.** Immunodetection of MMP-9 after GKS. (**A**–**F**) Representative photomicrographs of MMP-9 immunostaining after GKS. A few cells in the cortex of the sham-operated rats are MMP-9-positive (A and D). However, significant increases in MMP-9 expression levels occur in the irradiated cortex at 8 and 12 weeks after GKS (B, C). Low baseline levels of MMP-9 were observed in the contralateral cortex (E and F). Arrows indicate a positive MMP-9 signal. (**G**) The bar graph shows the temporal change of MMP-9 (+) cells after GKS. (**H**) Immunoblot analysis of MMP-9 protein expression in the damaged brain tissues from 1 to 12 weeks after GKS. (**I**) The bar graph shows the densitometric analysis of MMP-9-immunoreactive bands after GKS. The data are presented as the mean ± SD ($n = 4$, $^{*}P < 0.001$ when compared with the control group, $^{\#}P < 0.001$ when compared with the contralateral cortex). Scale bar: 50 μm.

be induced by ionizing irradiation and can contribute to the pathological process.

Our study shows that the levels of CD147 protein were significantly increased in the irradiated cortices after GKS. Double-staining techniques revealed that CD147 localized with endothelial cells and astrocytes. Recently, CD147 expression has been found in the cerebrum of mice [16] and in endothelial cells of the normal human brain [17]. Indeed, mice lacking the *CD147* gene have several neurological and cognitive defects and reduced BBB integrity [18]. Most studies have also demonstrated that the expression of CD147 is upregulated in a wide variety of CNS diseases. For example, in an animal model of experimental autoimmune encephalomyelitis, CD147 was shown to degrade components of the BBB, promoting leukocyte infiltration into the CNS [13]. In an animal model of transient ischemia, excessive expression of CD147 was associated with damage to the basal lamina [12]. Some researchers found that the CD147 molecule is highly expressed in CNS tumors, such as gliomas and pituitary adenomas, and is associated with tumor aggressiveness, invasiveness and poor prognosis [19, 20]. The experimental data have shown that the role of CD147 in pathological conditions is closely associated with the breakdown of tight junctions and the ECM [21, 22]; furthermore, the functional importance of CD147 is mainly related to its ability to induce MMPs, such as MMP-9 [23]. In the present study, increased MMP-9 expression was observed in irradiated brain tissue.

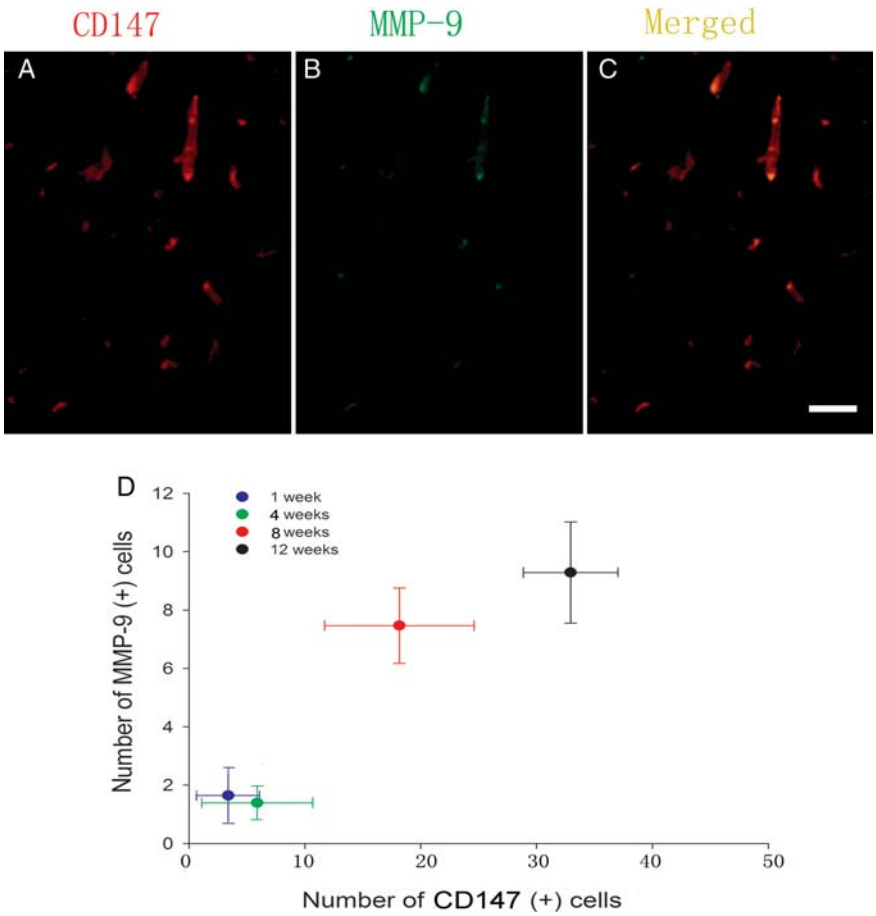


**Fig. 5.** The relationship between CD147 levels and MMP-9 expression. (**A**–**D**) Immunofluorescence double-staining for CD147 (red) and MMP-9 immunoreactivity (green) in the target region 12 weeks after radiosurgery. The colocalization of CD147 (A) with MMP-9 (B) was observed in the irradiated cortex (C, yellow). (D) Correlation between CD147-positive cells and MMP-9 expression in the irradiated cortex after GKS. Scale bar: 50 μm.

Interestingly, our results also showed that MMP-9 was colocalized with CD147, and MMP-9 was significantly correlated with CD147 in the brain of rats that received GKS. Our findings are similar to previous results in which ischemia-induced CD147 expression was correlated with MMP-9 and contributed to neurovascular remodeling in a mouse model of permanent middle cerebral artery occlusion [24]. Moreover, MMP-9 expression was increased after lung injury caused by ionizing irradiation, and it affected the structural integrity of lung tissue by degrading collagen IV of basement membranes [25]. Normally, MMPs are thought to play a key role in ECM degradation and remodeling. However, these proteases have been reported to contribute to endothelial cell injury [26]. A previous study has revealed that MMPs interrupt cell–matrix interactions and weaken the vessel wall by degrading tight junction proteins in injured brain tissue [27]. The proteolytic breakdown of the BBB vasculature increases the permeability of the barrier resulting in vasogenic edema, and this breakdown is thought to take an active part in the pathophysiology of CNS diseases [28]. The over-expression of CD147 and MMP-9 in irradiated brain tissues likely contributes to the abnormalities observed in vascular remodeling and the disruption of vascular integrity.

The mechanisms that underlie the increased expression of CD147/MMP-9 after GKS remain unknown. One possibility may be related to the up-regulation of cytokines in irradiated tissues. The irradiation could trigger a signaling cascade that develops during the clinically silent period. In this process, increased cytokines may exacerbate radiation-induced brain damage, such as the disruption of microvascular integrity. Studies have reported that increased CD147 levels in cancer cells are linked to the deregulation of epidermal growth factor receptor signaling [29]. The upregulation of CD147 expression in human corneal epithelial cells may be a response to transforming growth factor

stimulation [30]. These cytokines, which are potentially capable of influencing CD147 expression, were reported to be increased within irradiated tissue [31].

In summary, this study is the first to show a positive correlation between CD147 and MMP-9 expression levels after CNS radiation injury. Our results suggest that CD147 could be a potential candidate target for ameliorating GKS-induced brain injury.

## FUNDING

This work was supported by grants-in-aid for scientific research from the Tianjin Bureau of Public Health, Tianjin, China (Grant: 06KZ25, 2011KZ96).

## REFERENCES

1. Buis DR, Meijer OW, van den Berg R *et al*. Clinical outcome after repeated radiosurgery for brain arteriovenous malformations. *Radiother Oncol* 2010;**95**:250–6.
2. Dewan S, Norén G. Retreatment of vestibular schwannomas with Gamma Knife surgery. *J Neurosurg* 2008;**109**:144–8.
3. Friehs GM, Park MC, Goldman MA *et al*. Stereotactic radiosurgery for functional disorders. *Neurosurg Focus* 2007;**23**: E3.
4. Yuan H, Gaber MW, McColgan T *et al*. Radiation-induced permeability and leukocyte adhesion in the rat blood-brain barrier: modulation with anti-ICAM-1 antibodies. *Brain Res* 2003;**969**:59–69.
5. d'Avella D, Cicciarello R, Albiero F *et al*. Quantitative study of blood-brain barrier permeability changes after experimental whole-brain radiation. *Neurosurgery* 1992;**30**:30–4.
6. Gabison EE, Hoang-Xuan T, Mauviel A *et al*. EMMPRIN/CD147, an MMP modulator in cancer, development and tissue repair. *Biochimie* 2005;**87**:361–8.
7. Tang Y, Kesavan P, Nakada MT *et al*. Tumor-stroma interaction: positive feedback regulation of extracellular matrix metalloproteinase inducer (EMMPRIN) expression and matrix metalloproteinase-dependent generation of soluble EMMPRIN. *Mol Cancer Res* 2004;**2**:73–80.
8. Bougatef F, Quemener C, Kellouche S *et al*. EMMPRIN promotes angiogenesis through hypoxia-inducible factor-2alpha-mediated regulation of soluble VEGF isoforms and their receptor VEGFR-2. *Blood* 2009;**114**:5547–56.
9. Hawkins BT, Lundeen TF, Norwood KM *et al*. Increased blood-brain barrier permeability and altered tight junctions in experimental diabetes in the rat: contribution of hyperglycaemia and matrix metalloproteinases. *Diabetologia* 2007;**50**:202–11.
10. Gasche Y, Copin JC, Sugawara T *et al*. Matrix metalloproteinase inhibition prevents oxidative stress-associated blood-brain barrier disruption after transient focal cerebral ischemia. *J Cereb Blood Flow Metab* 2001;**21**:1393–400.
11. Yang X, Zhang P, Ma Q *et al*. EMMPRIN contributes to the in vitro invasion of human salivary adenoid cystic carcinoma cells. *Oncol Rep* 2012;**27**:1123–7.
12. Burggraf D, Liebetrau M, Martens HK *et al*. Matrix metalloproteinase induction by EMMPRIN in experimental focal cerebral ischemia. *Eur J Neurosci* 2005;**22**:273–7.
13. Agrawal SM, Silva C, Tourtellotte WW *et al*. EMMPRIN: a novel regulator of leukocyte transmigration into the CNS in multiple sclerosis and experimental autoimmune encephalomyelitis. *J Neurosci* 2011;**31**:669–77.
14. Kamiryo T, Kassell NF, Thai QA *et al*. Histological changes in the normal rat brain after gamma irradiation. *Acta Neurochir (Wien)* 1996;**138**:451–9.
15. Paxinos G, Watson C. *The Rat Brain in Sterotaxic Coordinates*, 2nd edn. Florida: Academic Press, 1986.
16. Nakai M, Chen L, Nowak RA *et al*. Tissue distribution of basigin and monocarboxylate transporter 1 in the adult male mouse: a study using the wild-type and basigin gene knockout mice. *Anat Rec A Discov Mol Cell Evol Biol* 2006;**288**:527–35.
17. Sameshima T, Nabeshima K, Toole BP *et al*. Expression of emmprin (CD147), a cell surface inducer of matrix metalloproteinases, in normal human brain and gliomas. *Int J Cancer* 2000;**88**:21–7.
18. Igakura T, Kadomatsu K, Taguchi O *et al*. Roles of basigin, a member of the immunoglobulin superfamily, in behavior as to an irritating odor, lymphocyte response, and blood-brain barrier. *Biochem Biophys Res Commun* 1996;**224**:33–6.
19. Gu J, Zhang C, Chen R *et al*. Clinical implications and prognostic value of EMMPRIN/CD147 and MMP2 expression in pediatric gliomas. *Eur J Pediatr* 2009;**168**:705–10.
20. Zhang Y, He N, Zhou J *et al*. The relationship between MRI invasive features and expression of EMMPRIN, galectin-3, and microvessel density in pituitary adenoma. *Clin Imaging* 2011;**35**:165–73.
21. Huet E, Gabison EE, Mourah S *et al*. Role of emmprin/CD147 in tissue remodeling. *Connect Tissue Res* 2008;**49**:175–9.
22. Huet E, Vallée B, Delbé J *et al*. EMMPRIN modulates epithelial barrier function through a MMP-mediated occludin cleavage: implications in dry eye disease. *Am J Pathol* 2011;**179**:1278–86.
23. Jouneau S, Khorasani N, DE Souza P *et al*. EMMPRIN (CD147) regulation of MMP-9 in bronchial epithelial cells in COPD. *Respirology* 2011;**16**:705–12.
24. Zhu W, Khachi S, Hao Q *et al*. Upregulation of EMMPRIN after permanent focal cerebral ischemia. *Neurochem Int* 2008;**52**:1086–91.
25. Yang K, Palm J, König J *et al*. Matrix-Metallo-Proteinases and their tissue inhibitors in radiation-induced lung injury. *Int J Radiat Biol* 2007;**83**:665–76.
26. Boehme MW, Galle P, Stremmel W. Kinetics of thrombomodulin release and endothelial cell injury by neutrophil-derived proteases and oxygen radicals. *Immunology* 2002;**107**:340–9.
27. Yang Y, Rosenberg GA. MMP-mediated disruption of claudin-5 in the blood-brain barrier of rat brain after cerebral ischemia. *Methods Mol Biol* 2011;**762**:333–45.
28. Rosenberg GA, Cunningham LA, Wallace J *et al*. Immunohistochemistry of matrix metalloproteinases in reperfusion injury to rat brain: activation of MMP-9 linked to stromelysin-1 and microglia in cell cultures. *Brain Res* 2001;**893**:104–12.

29. Menashi S, Serova M, Ma L *et al*. Regulation of extracellular matrix metalloproteinase inducer and matrix metalloproteinase expression by amphiregulin in transformed human breast epithelial cells. *Cancer Res* 2003;**63**:7575–80.
30. Gabison EE, Mourah S, Steinfels E *et al*. Differential expression of extracellular matrix metalloproteinase inducer (CD147) in normal and ulcerated corneas: role in epithelio-stromal interactions and matrix metalloproteinase induction. *Am J Pathol* 2005;**166**:209–19.
31. Dent P, Yacoub A, Contessa J *et al*. Stress and radiation-induced activation of multiple intracellular signaling pathways. *Radiat Res* 2003;**159**:283–300.